2011

Analytic & Numerical Study of a Vortex Motion Equation

Daniel Bueller
University of Central Florida

Analytic & Numerical Study of a Vortex Motion Equation

by

Daniel Bueller
B.S. Clearwater Christian College, 2009
A.A. Saint Petersburg College, 2006

A thesis submitted in partial fulfillment of the requirements
for the degree of Master of Science
in the Department of Mathematics
in the College of Sciences
at the University of Central Florida
Orlando, Florida

Spring Term
2011

Major Professor: David Rollins

Abstract

A nonlinear second order differential equation related to vortex motion is derived. This equation is analyzed using various numerical and analytical techniques including finding approximate solutions using a perturbative approach.

This thesis is dedicated to my wife: for all of her love and support.

Acknowledgments

I would like to first thank Dr. Rollins for being a professor very involved in my maturing as a first year graduate student as well as his guidance in overseeing my research ever since. I would also like to thank Dr. Mohapatra and Dr. Moore for serving on my thesis committee and being available to give assistance and feedback along the way. A special thank you goes out to Dr. Li and the mathematics staff who have been there from day one to support me and answer countless of logistical questions. Lastly I would like to acknowledge the professors and fellow graduate students who have imparted to me immense amounts of mathematical enrichment over my graduate experience.

TABLE OF CONTENTS

LIST OF FIGURES

CHAPTER 1
INTRODUCTION AND DERIVATION

1.1 Introduction to Vortex Motion and Superfluid ^{4}He

We first give a concise overview of the physical topics in which we are about to explore. Let us first introduce vortices and a few of their many appearances in various phenomena. According to H. Lamb [8], a line drawn from point to point so that its direction is everywhere that of the instantaneous axis of rotation of the fluid is called a vortex-line. If through every point of a small closed curve we draw the corresponding vortex-line, we obtain a tube, which is called a vortex-tube. The fluid contained within such a tube constitutes what is called a vortex-filament, or simply a vortex. Put simply, a vortex is a rotating flow of fluid; the motion of the fluid spinning rapidly around a center is called a vortex. I. Kroo [7] asserts that a vortex filament may be visualized as a thin tube in which the flow has vorticity, ω (the tendency for elements of the fluid to spin).

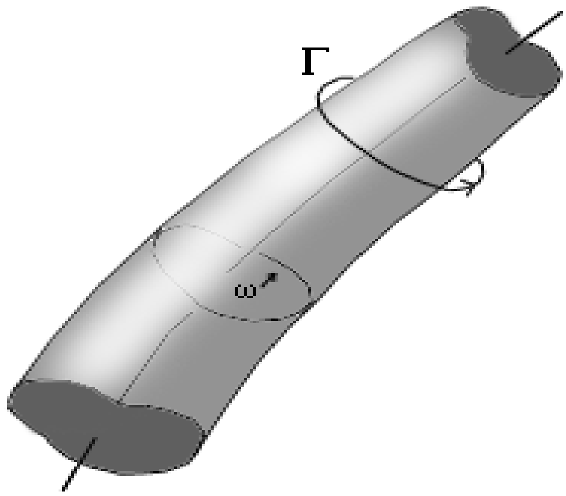

Figure 1.1: Vortex filament

As the diameter is made small, but the circulation, Γ, is held fixed, this region of vorticity is called a vortex filament. An illustration is also provided by I. Kroo which we have reproduced in Figure 1.1 [7]. Such phenomena occur in various avenues including tornadic activity, airplane wings and propellers, and of interest to us, in superfluid.

Now we will discuss the topic of superfluid liquid helium-4 or ^{4}He. Liquid ^{4}He is comprised of a normal fluid state helium I above a specific temperature and a superfluid state helium II below that temperature. The temperature at which this transition occurs is at about 2.2 K; this is called the λ-point (Bunch, [2].) We are mostly interested in the superfluid phase. Superfluids have properties very distinct to that of normal fluids. For instance, the superfluids ^{3}He and ^{4}He are the only liquids which do not solidify even at absolute zero temperature, (Volovik, [15].) Another distinct phenomena of superfluids is that they are said to be made up of two components: a normal component which is viscous and a superfluid component which has zero viscosity (Leitner, [10].) D.S. Viswanath [14] observes that when a liquid flows, it has an internal resistance to flow. Viscosity is a measure of this resistance to flow. In other words, the more viscous the fluid is, the greater its difficulty of movement. Since superfluid ^{4}He has a zero viscosity component, it can essentially defy gravity and creep up the walls of an object to form a thin film called the Rollin film (Leitner, [10].) This phenomena is shown in Figure 1.2.

(a) Superfluid exiting a medium

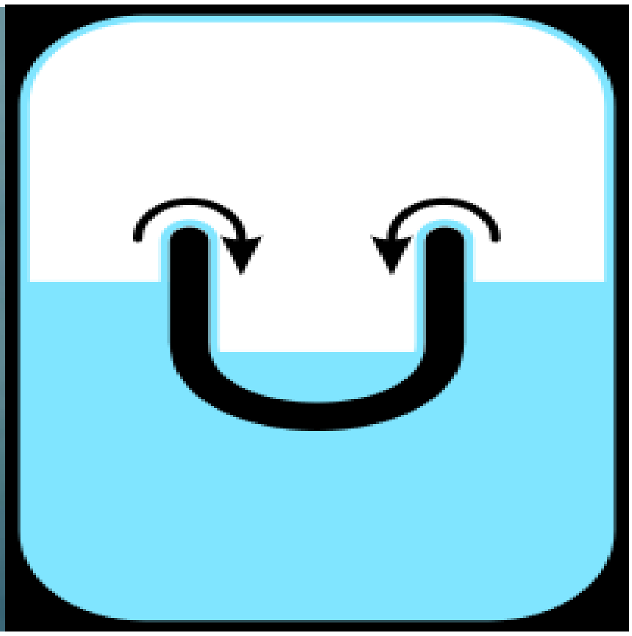

(b) Superfluid entering a medium

Figure 1.2: Rollin Film

1.2 Derivation of System

B.K. Shivamoggi [12] considers that upon including the effect of the frictional force exerted by the normal fluid on a vortex line, the self-induced velocity $\mathbf{v}$ of the vortex line in the reference frame moving with the superfluid according to the local induction approximation is given by the Hall-Vinen equation

$$\mathbf{v} = \gamma\kappa\hat{\mathbf{T}} \times \hat{\mathbf{N}} + \alpha\hat{\mathbf{T}} \times (\mathbf{U} - \gamma\kappa\hat{\mathbf{T}} \times \hat{\mathbf{N}}) - \alpha'\hat{\mathbf{T}} \times [\hat{\mathbf{T}} \times (\mathbf{U} - \gamma\kappa\hat{\mathbf{T}} \times \hat{\mathbf{N}})]. \tag{1.1}$$

Here we have defined the friction coefficients to be α and α', which are usually found to be small except near the λ-point. γ is a constant related to the quantum of circulation and the effective core radius of the filament. We recognize the average curvature as κ, while the unit tangent and unit normal vectors to the vortex filament are $\hat{\mathbf{T}}$ and $\hat{\mathbf{N}}$ respectively. Lastly, $\mathbf{U}$ is the normal fluid velocity taken to be constant in space and time and prescribed [12]. In this paper we will, like B.K. Shivamoggi [12], consider the vortex essentially aligned along the x-axis with $\mathbf{U} = U_1\hat{\mathbf{i}} + U_2\hat{\mathbf{j}} + U_3\hat{\mathbf{k}}$, then equation (1.1) becomes

$$\mathbf{v} = (1-\alpha')\gamma\kappa\hat{\mathbf{T}} \times \hat{\mathbf{N}} + \alpha\hat{\mathbf{T}} \times \mathbf{U} + \alpha\gamma\kappa\hat{\mathbf{N}} - \alpha' U_1\hat{\mathbf{T}}. \tag{1.2}$$

Consider a vortex line parametrized by x of the form $y = y(x)$ lying in a plane which is rotated with angular velocity Ω [12], so we will have $\mathbf{r} =< x, y(x), 0 >$. Please take note that for the remainder of this paper we will resort to ordered set notation when referencing vectors rather than labeling them $\hat{\mathbf{i}}$, $\hat{\mathbf{j}}$, and $\hat{\mathbf{k}}$. Now recall the following definitions (Larson, [9]) for the unit tangent vector, unit normal vector, and curvature

$$\hat{\mathbf{T}} = \frac{\mathbf{r}'}{||\mathbf{r}'||} \tag{1.3}$$

$$\hat{\mathbf{N}} = \frac{\hat{\mathbf{T}}'}{||\hat{\mathbf{T}}'||} \tag{1.4}$$

$$\kappa = \frac{||\hat{\mathbf{T}}'||}{||\mathbf{r}'||} \tag{1.5}$$

where prime denotes differentiation with respect to x. Evaluating equations (1.3), (1.4), and (1.5) give the following

$$\hat{\mathbf{T}} = \frac{< 1, y_x, 0 >}{(1+y_x^2)^{1/2}} \tag{1.6}$$

$$\hat{\mathbf{N}} = \frac{< -y_x, 1, 0 >}{(1+y_x^2)^{1/2}} \tag{1.7}$$

$$\kappa = \frac{y_{xx}}{(1+y_x^2)^{3/2}}. \tag{1.8}$$

Assuming the velocity is in the x direction only, that is $\mathbf{U} =< U_1, 0, 0 >$, preforming the appropriate cross products, and substituting into equation (1.2) yields

$$\begin{aligned} \mathbf{v} &= (1-\alpha')\gamma\frac{y_{xx}}{(1+y_x^2)^{3/2}} < 0,0,1 > +\alpha\frac{-U_1}{(1+y_x^2)^{1/2}} < 0,0,y_x > \\ &\quad + \alpha\gamma\frac{y_{xx}}{(1+y_x^2)^2} < -y_x, 1, 0 > -\alpha'\frac{U_1}{(1+y_x^2)^{1/2}} < 1, y_x, 0 > . \end{aligned}$$

Substituting in angular velocity $\mathbf{v} = \Omega y \hat{\mathbf{k}}$ and taking the z direction we obtain

$$-\Omega y = (1-\alpha')\gamma\frac{y_{xx}}{(1+y_x^2)^{3/2}} - \alpha U_1\frac{y_x}{(1+y_x^2)^{1/2}}. \tag{1.9}$$

We can renormalize the vortex strength γ so that (1.9) can be written as

$$-\Omega y = \gamma\frac{y_{xx}}{(1+y_x^2)^{3/2}} - \alpha U_1\frac{y_x}{(1+y_x^2)^{1/2}} \tag{1.10}$$

and put $y_x = \tan\theta$ so θ is the angle between the tangent to the vortex and the x-axis (Shivamoggi, [12])

$$\begin{aligned} -\Omega y &= \gamma\frac{y_{xx}}{(1+\tan^2\theta)^{3/2}} - \alpha U_1\frac{\tan\theta}{(1+\tan^2\theta)^{1/2}} \\ -\Omega y &= \gamma\frac{y_{xx}}{\sec^3\theta} - \alpha U_1\sin\theta. \end{aligned} \tag{1.11}$$

To continue with the transformation of equation (1.9) we apply the chain rule to find y_{xx}. During this transformation we will also need to recall the arc length definition $\frac{\mathrm{d}s}{\mathrm{d}x} = ||\mathbf{r}'(x)||$ from [9].

$$\frac{\mathrm{d}^2 y}{\mathrm{d}x^2} = \frac{\mathrm{d}s}{\mathrm{d}x}\,\frac{\mathrm{d}}{\mathrm{d}s}\left(\frac{\mathrm{d}y}{\mathrm{d}x}\right) = \sqrt{1+y_x^2}\,\frac{\mathrm{d}}{\mathrm{d}s}(\tan\theta) = \sqrt{1+\tan^2\theta}\ \sec^2\theta\,\frac{\mathrm{d}\theta}{\mathrm{d}s}$$

$$y_{xx} = \sec^3\theta\,\frac{\mathrm{d}\theta}{\mathrm{d}s} \tag{1.12}$$

Now substituting (1.12) into (1.11) gives

$$\gamma\frac{\mathrm{d}\theta}{\mathrm{d}s} - \alpha U_1 \sin\theta = -\Omega y \tag{1.13}$$

After differentiating equation (1.13) with respect to arc length, we obtain the following nonlinear differential equation

$$\begin{aligned} \frac{\mathrm{d}}{\mathrm{d}s}\left[\gamma\frac{\mathrm{d}\theta}{\mathrm{d}s} - \alpha U_1\sin\theta + \Omega y\right] &= 0 \\ \gamma\frac{\mathrm{d}^2\theta}{\mathrm{d}s^2} - \alpha U_1 \cos\theta\,\frac{\mathrm{d}\theta}{\mathrm{d}s} + \Omega\frac{\mathrm{d}y}{\mathrm{d}s} &= 0. \end{aligned} \tag{1.14}$$

Recall that we let $y_x = \tan\theta$. We will once more apply the chain rule

$$\begin{aligned} \frac{\mathrm{d}y}{\mathrm{d}x} &= \frac{\mathrm{d}y}{\mathrm{d}s}\,\frac{\mathrm{d}s}{\mathrm{d}x} \\ \tan\theta &= \sec\theta\,\frac{\mathrm{d}y}{\mathrm{d}s} \\ \sin\theta &= \frac{\mathrm{d}y}{\mathrm{d}s}. \end{aligned} \tag{1.15}$$

Finally we can substitute equation (1.15) into (1.14) to obtain

$$\gamma\frac{\mathrm{d}^2\theta}{\mathrm{d}s^2} - \alpha U_1\cos\theta\,\frac{\mathrm{d}\theta}{\mathrm{d}s} + \Omega\sin\theta = 0. \tag{1.16}$$

We recognize that equation (1.16) is a modification of the pendulum equation when $U_1 = 0$

$$\gamma \frac{\mathrm{d}^2\theta}{\mathrm{d}s^2} + \Omega \sin\theta = 0. \tag{1.17}$$

The solutions of the pendulum equation (1.17) are Jacobi elliptic functions which are periodic in s. Equation (1.17) will be revisited in relation to equation (1.16) briefly in Chapter 2 and again at length in Chapter 3.

1.3 Summary of Introduction

In Section 1.1 we discussed some of the major physical topics involved in vortex motion and superfluid; in the previous section we studied the mathematics that lead up to the derivation of the equation of interest. In Chapters 2 and 3 we will do extensive mathematical analysis of the equation given in (1.16) to discover its different properties. In Chapter 4 we shall attempt to find a new perturbation approximation of the equation that retains the properties found in Chapters 2 and 3. In the final chapter we shall conclude by discussing and recounting our results and their potential for furter research in vortex motion.

CHAPTER 2
STABILITY OF EQUILIBRIUM SOLUTIONS

2.1 Stability Analysis

In the introduction we derived equation (1.16), we now wish to examine the stability of the solutions of the initial valued nonlinear ordinary differential equation

$$\begin{cases} \theta'' + a\cos\theta\,\theta' + b\sin\theta = 0, \quad a \neq 0, b > 0 \\ \\ \theta(0) = c \qquad \theta'(0) = d \end{cases} \tag{2.1}$$

where the constants a and b have been re-defined by scaling (1.16) as $a = -\frac{\alpha U_1}{\gamma}$ and $b = \frac{\Omega}{\gamma}$; c and d are initial conditions on θ. We note that a may be positive or negative depending on the sign of the velocity term U_1 while b is strictly positive. Also note that we are now using prime notation instead of differential operators where prime denotes differentiation with respect to s. To analyze linear stability, we write this nonlinear differential equation as a system of first order differential equations. Let

$$\begin{array}{rcl} x &=& \theta \\ y &=& \theta' \end{array}. \tag{2.2}$$

Differentiating both sides of (2.2) with respect to time and solving for θ'' from (2.1) yields the system.

$$\begin{aligned} x' &= y && (2.3) \\ y' &= -a\cos x\, y - b\sin x && (2.4) \end{aligned}$$

The equilibrium solutions are found by setting the equations in (2.3) and (2.4) equal to zero

$$\begin{aligned} 0 &= y \\ 0 &= -a\cos x\, y - b\sin x \end{aligned}$$

we see that y must be 0 which leaves us with

$$0 = -b\sin x. \tag{2.5}$$

Since b is nonzero, our equilibrium solutions are

$$(n\pi, 0),\ \ n \in \mathbb{Z}. \tag{2.6}$$

Now that we have found our equilibrium points, we now wish to analyze the stability of these solutions. To do this, we find the Jacobian matrix of the equations we formulated in (2.3) and (2.4).

$$J = \begin{pmatrix} 0 & 1 \\ ay\sin x - b\cos x & -a\cos x \end{pmatrix} \tag{2.7}$$

2.1.1 Case I - Real Eigenvalues (n even)

Evaluating the matrix from (2.7) at our equilibrium points when n is even gives

$$J = \begin{pmatrix} 0 & 1 \\ -b & -a \end{pmatrix}. \tag{2.8}$$

Now consider the following process of finding eigenvalues of this matrix

$$0 = |J - \lambda I| = \lambda^2 + a\lambda + b.$$

Then by making use of the Quadratic Formula

$$\lambda = \frac{-a \pm \sqrt{a^2 - 4b}}{2}. \tag{2.9}$$

If we take $0 < 4b < a^2$, then we will obtain from (2.9) two real eigenvalues. Let us, without loss of generality, choose λ_1 to be the smaller of the two eigenvalues and λ_2 to be the larger; we will continue to make this generalization, where possible, throughout the duration of this paper. We see that even inside this case we have two subcases; if $a < 0$ then $\lambda_1, \lambda_2 > 0$, but if $a > 0$ then $\lambda_1, \lambda_2 < 0$.

Using some basic ordinary differential equation stability theory [5], we observe that in the case that λ_1 and λ_2 are negative we have stable solutions whereas when the eigenvalues are positive we acquire unstable solutions at the equilibrium points. In summary of this case we should expect to see stable solutions at $(n\pi, 0)$, for even integer values of n, when $a > 0$ and unstable solutions when $a < 0$.

2.1.2 Case II - Complex Eigenvalues (n even)

Consider again equation (2.9), but now take $4b > a^2$. This will force the discriminant to be negative, thus giving complex conjugate eigenvalues

$$\lambda = -\frac{a}{2} \pm \frac{i}{2}\sqrt{4b - a^2}. \tag{2.10}$$

We see that the real part of these eigenvalues depend on a; if $a < 0$ then $\Re(\lambda) > 0$, but if $a > 0$ then $\Re(\lambda) < 0$. Again we reference Grimshaw [5] and note that when the real part of the eigenvalues in (2.10) are negative we have stable spiral solutions whereas when the real part is positive we obtain unstable spiral solutions at the equilibrium points.

2.1.3 Case III - n odd

When evaluating the Jacobian matrix given in (2.7) at the equilibrium points found in (2.6) for odd integers of n, we obtain

$$J = \begin{pmatrix} 0 & 1 \\ b & a \end{pmatrix}. \tag{2.11}$$

Following a similar process for finding eigenvalues as we did previously, we come to the following result

$$0 = |J - \lambda I| = \lambda^2 + a\lambda - b$$

$$\lambda = \frac{a \pm \sqrt{a^2 + 4b}}{2}. \tag{2.12}$$

Since $a, b \in \mathbb{R}$ and $b > 0$, $\lambda_1 < 0 < \lambda_2$ $\forall$ values of a and b. Thus we obtain saddle points at equilibrium points $(n\pi,\, 0)$ for odd integer values of n.

Having obtained saddle points, one topic of interest would be the orientation of the trajectories. We can examine which solutions begin far away from the saddle then grow closer and which do the opposite by observing the eigenvectors X_k associated with the eigenvalues λ_k, for $k = 1,\, 2$.

$$\begin{aligned}
0 &= (J - \lambda_k I)X_k \\
\begin{pmatrix} 0 \\ 0 \end{pmatrix} &= \begin{pmatrix} -\lambda_k & 1 \\ b & a-\lambda_k \end{pmatrix} \begin{pmatrix} X_k \\ Y_k \end{pmatrix} \\
&\begin{cases} 0 = -\lambda_k X_k + Y_k \\ 0 = bX_k + (a-\lambda_k)Y_k \end{cases} \\
&\begin{cases} Y_k = \lambda_k X_k \\ Y_k = -\frac{b}{a-\lambda_k} X_k \end{cases}
\end{aligned} \tag{2.13}$$

So we see that when we use λ_1 we will obtain a line with a negative slope whereas when we choose λ_2 we obtain a line with a positive slope. This leads us to conclude that the solution with positive slope running through the saddle point is unstable while the other approaches the saddle point as $t \to \infty$.

All three of the cases just discussed will be further illustrated by phase plane plots in the coming sections.

2.2 The Phase Plane

We have already alluded to the language of phase plans and trajectories, but now we will define and analyze these topics in a more formal way. Consider the following general first order system of equation

$$\begin{cases} x' = F(x, y) \\ y' = G(x, y) \\ x(t_0) = \alpha, \ \ y(t_0) = \beta \end{cases} . \tag{2.14}$$

L.C. Andrews [1] considers the solution functions $x = x(t)$ and $y = y(t)$ of (2.14) as parametric equations of an arc in the xy-plane that passes through the point (α, β) The xy-plane is then called the phase plane. L.C. Andrews [1] continues by stating that any arc described parametrically by a solution of (2.14) is called a trajectory, with the positive direction along the trajectory defined by the direction of increasing t. By eliminating the parameter t we can find the trajectories. Taking the ratio of the two equations in (2.14) is one way to eliminate t

$$\frac{y'}{x'} = \frac{dy}{dx} = \frac{G(x, y)}{F(x, y)}. \tag{2.15}$$

The solutions of (2.15) are the trajectories. Thus for equation (2.1) we have

$$\frac{dy}{dx} = -\frac{a \cos x \, y + b \sin x}{y}. \tag{2.16}$$

2.3 Numerical Solutions

To illustrate numerically the results we found in the previous two sections we did some implementation using MATLAB. First we needed to create an .m file that modeled equation (2.1). To do this we referred to the first order equations that we formulated in (2.3) and (2.4) and formed a matrix $U = (x', y')$.

To create the phase plane we used a MATLAB function called phasePlane which calls the functions RungeKutta and RKStep; all of which were created by a fellow University of Central Florida graduate student, Johann Veras. As the name would indicate the RungeKutta function employs the Runge–Kutta forth order method of solving ordinary differential equations. We then created a row vector that represented the initial values of the system; this vector contained thirty four points. We chose these points in a careful systematic way such that the plots would fill the display in an orderly and symmetric pattern. Finding the eigenvectors from (2.13) proved helpful numerically as well because we were able to choose initial values very close to the saddle point which gave us very accurate plots around these equilibrium points; four of the thirty four points were dedicated to this purpose. Finally we chose our time interval T to be an interval of values ranging from an initial time of 0 and final time of 1000 and the number of points for which the system was to be computed on, 10000.

The following figure is the product of the phasePlane function.

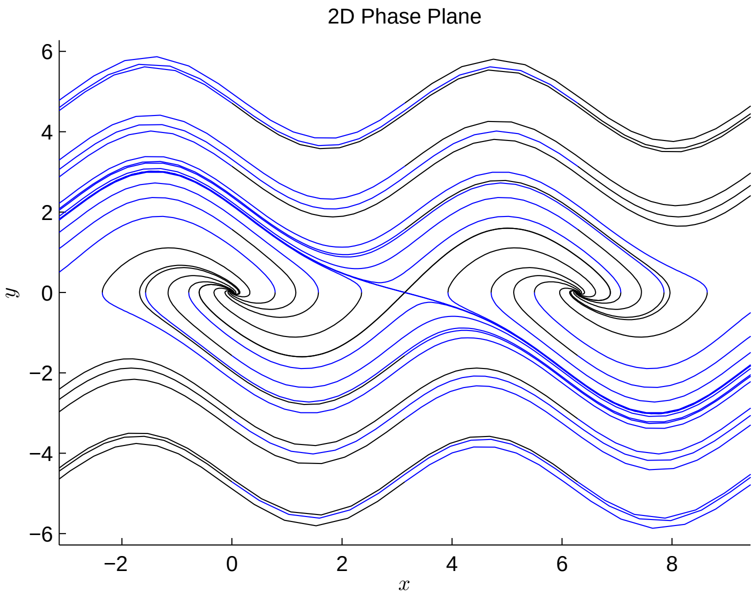

Figure 2.1: Phase plane where $a = 1$, $b = \frac{1}{2}$; $\quad 4b > a^2$

The function not only computes solutions going forward in time on the specified interval, but solutions moving backward in time as well. The black lines indicate moving forward in time while the blue denotes negative time. This trend will continue for all phase plane plots in this paper. Upon close observation, one may notice where lines pass from black to blue; such areas are the initial values that we chose to formulate the plot.

From Figure 2.1 we note that the equilibrium points appear to lie on $(n\pi, 0)$. It also is clear that when n is even that the said equilibrium points are stable spirals and when n is odd the equilibrium points form saddle points. As the caption in Figure 2.1 indicates, we are looking at the case when $4b > a^2$, thus from Section 2.1.2 we expected stable spirals;

hence, all of our numerical analysis and implementation agrees with the analysis preformed in Section 2.1 thus far.

The following figure shows the case where $0 < 4b < a^2$.

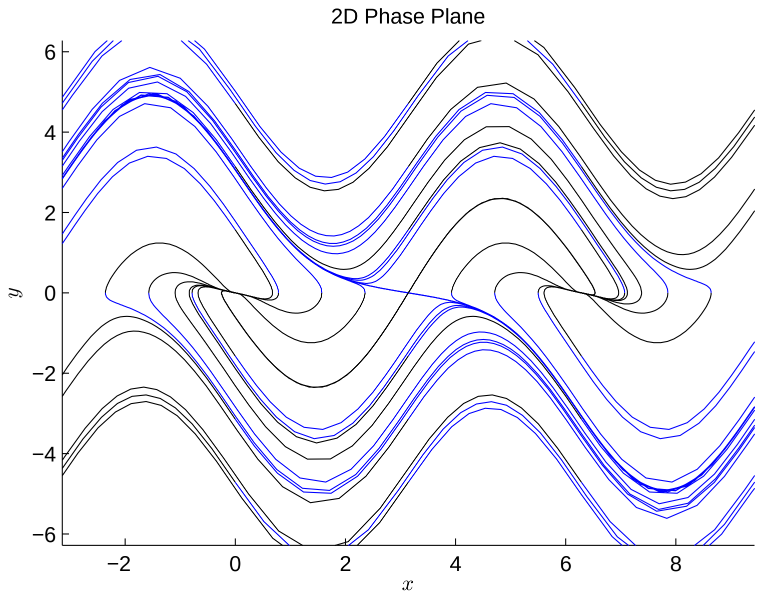

Figure 2.2: Phase plane where $a = 2$, $b = \frac{1}{2}$; $\quad 0 < 4b < a^2$

The major difference between the plot in Figure 2.1 and that of Figure 2.2 is that Figure 2.2's plot has stable solutions; whereas, Figure 2.1 has stable spiral solutions.

It should be noted that if there were no damping term on equation (2.1), then we would have the well documented pendulum equation. With this in mind we found it of interest to see how the system behaves when the damping term a took on small values. In Chapter 4 we will take a more formal analytic approach in examining certain perturbations.

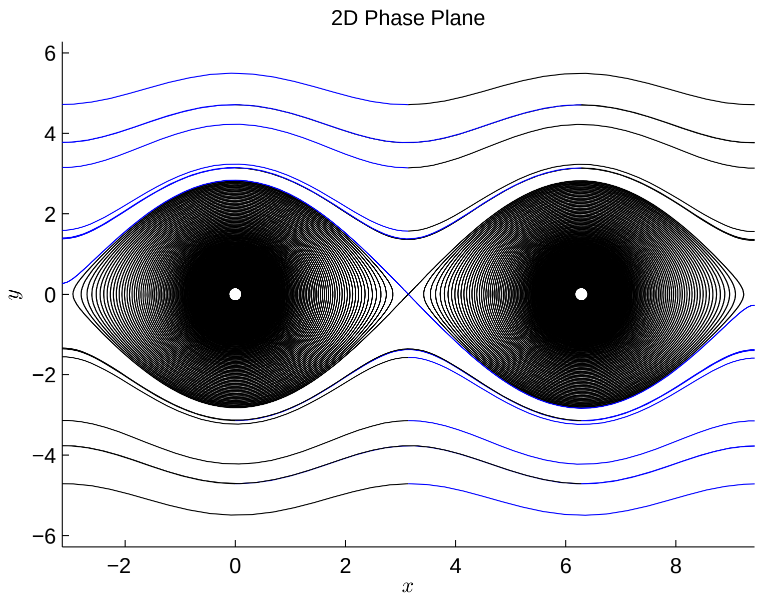

Figure 2.3: Phase plane where $a = \frac{1}{100}$, $b = 2$; $\quad 4b > a^2$

The solutions of this phase plane look very much like those of a pendulum equation which is shown in Figure 2.4. The major difference between the plots produced for $a = \frac{1}{100}$ and $a = 0$ is that Figure 2.3 contains stable spirals while Figure 2.4 produces centres at $(n\pi, 0)$.

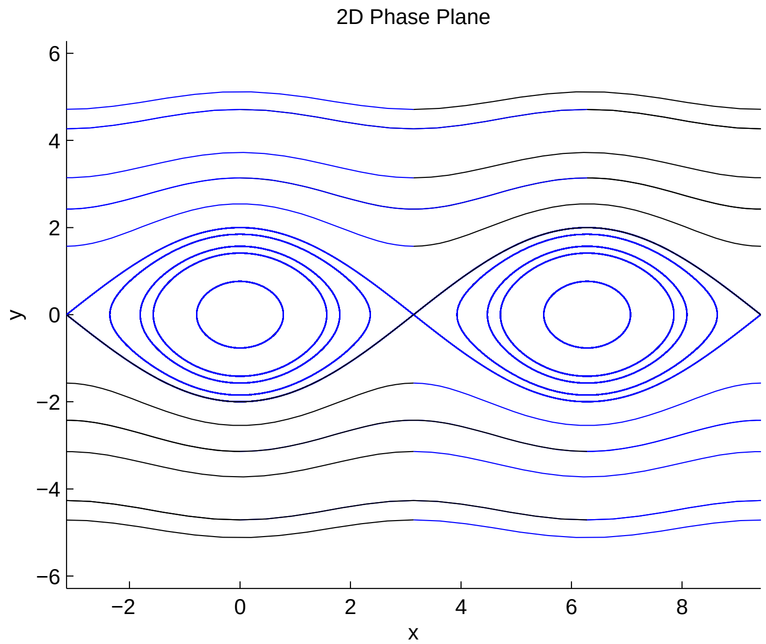

Figure 2.4: Phase plane of pendulum equation

Since we know that the pendulum equation has periodic solutions and it looks and behaves very much like equation (2.1) for small values of a, we became interested in the periodicity of solutions to equation (2.1). This will be discussed in much detail in Chapter 3

2.4 Additional Plots

Let us recall the implicit substitution for the coefficient of the cosine term that we made when we moved from equation (1.16) to equation (2.1): $a = -\frac{\alpha U_1}{\gamma}$. We have simply called the damping coefficient a for the majority of this paper, but when we consider that a contains U_1, the normal fluid velocity, we see that we should consider plots were a is negative.

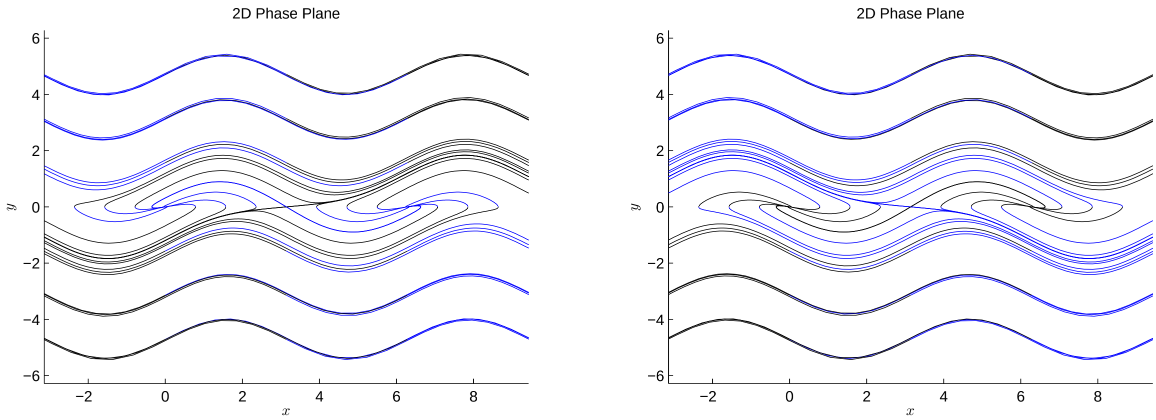

(a) $a < 0$

(b) $a > 0$

Figure 2.5: Phase plane where $a = \pm\frac{7}{10}$, $b = \frac{1}{10}$; $\quad 0 < 4b < a^2$

Please take note of the earlier distinction made between the blue lines and the black lines; the blue lines move backward in time and the black lines move forward in time. We can see the instability in Figure 2.5a, at $(n\pi, 0)$ for n even, that was initially discussed in Section 2.1.1. Figure 2.5b was plotted to show the contrast between the stability when $a > 0$ versus the instability when $a < 0$. It is also worth noting that these plots are of the case of stable/unstable solutions as opposed to stable/unstable spiral solutions, but since the difference between $4b$ and a^2 is so small it becomes slightly ambiguous to tell whether the stable/unstable solutions are spiraling or not. Figure 2.6 illustrates a plot for $a < 0$ with unstable spirals.

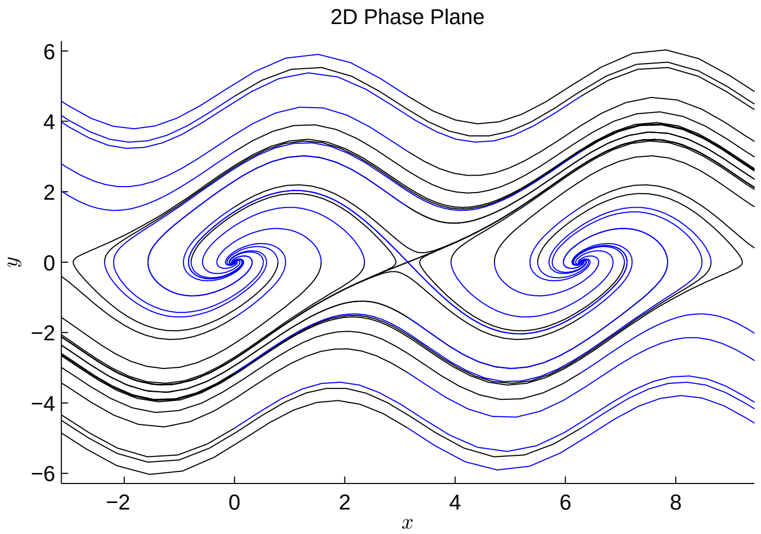

Figure 2.6: Phase plane where $a = -1$, $b = 1$; $\quad 4b > a^2$

We also observed some plots in which the values of a and b were much larger in comparison to the previous plots. Such plots exhibited behavior similar in nature, thus it would be redundant to produce such a plot here.

CHAPTER 3
ANALYSIS OF PERIODICITY

3.1 Hamiltonian Systems

In Section 2.3 we briefly compared the characteristics of equation (2.1) with the pendulum equation using Figures 2.3 and 2.4. Graphically, the phase planes looked very similar when the coefficient a of the damping term $a\cos\theta\,\theta'$ was small. As we began to mention in Chapter 2, the periodicity of solutions of equation (2.1) became a topic of interest because of the similarity to the pendulum equation which has periodic solutions and is characterized as a Hamiltonian system.

Definition 1. (Grimshaw, [5]) A Hamiltonian system is one for which the equations can be obtained from a single scalar function, $H(x, y)$, called the Hamiltonian. The system of equations is of the form

$$x' = \frac{\partial H}{\partial y}(x, y), \quad y' = -\frac{\partial H}{\partial x}(x, y). \tag{3.1}$$

An important property of autonomous Hamiltonian systems is that they are said to be conservative [5]. Consider

$$
\begin{aligned}
H' &= \frac{\partial H}{\partial y} y' + \frac{\partial H}{\partial x} x' \\
&= \frac{\partial H}{\partial y}\left(-\frac{\partial H}{\partial x}\right) + \frac{\partial H}{\partial x}\left(\frac{\partial H}{\partial y}\right) = 0,
\end{aligned}
$$

thus we see that $H =$ constant on its trajectories.

Consider the pendulum equation obtained from equation (2.1) by letting $a = 0$. For the sake of consistency, let us use the substitution used in (2.2) and write the equation as

$$x'' + b \sin x = 0. \tag{3.2}$$

To put equation (3.2) into the Hamiltonian form, let $y = x'$. Then (3.2) becomes

$$x' = y, \quad y' = -b \sin x.$$

This has the Hamiltonian form (3.1) if we define the Hamiltonian to be

$$H(x, y) = \frac{1}{2} y^2 - b \cos x. \tag{3.3}$$

3.2 Nearly Hamiltonian

We will now attempt to put equation (2.1) into the Hamiltonian form; let $y = x'$. Equation (2.1) becomes

$$x' = y, \quad y' = -ay \cos x - b \sin x.$$

By integrating we obtain

$$H(x,y) = \frac{1}{2}y^2 + ay\sin x - b\cos x,$$

which presents a problem because this does not preserve the required property that $x' = \frac{\partial H}{\partial y}(x,y)$ and $y' = -\frac{\partial H}{\partial x}(x,y)$. Thus, we cannot write equation (2.1) in such a way that it would have a Hamiltonian form, but we would like to see if it can be characterized as a nearly Hamiltonian system. A system is informally said to be nearly Hamiltonian if it is a perturbation of a Hamiltonian system that preserves the periodic nature of the original Hamiltonian system. P. Glendinning [4] considers a perturbation of a Hamiltonian system,

$$x' = f_1(x,y) + \epsilon g_1(x,y), \quad f_1(x,y) = \frac{\partial H}{\partial y}(x,y) \tag{3.4}$$

$$y' = f_2(x,y) + \epsilon g_2(x,y), \quad f_2(x,y) = -\frac{\partial H}{\partial x}(x,y) \tag{3.5}$$

and states that if Γ_ϵ is a periodic orbit for this perturbed equation, then we must have

$$\int_{\Gamma_\epsilon} \mathrm{d}H = 0 \tag{3.6}$$

since Γ_ϵ is a closed curve. But $\mathrm{d}H = (\frac{\partial H}{\partial x})\mathrm{d}x + (\frac{\partial H}{\partial y})\mathrm{d}y$ and thus

$$\int_{\Gamma_\epsilon} ((-y' + \epsilon g_2(x,y))\,\mathrm{d}x + (x' - \epsilon g_1(x,y))\,\mathrm{d}y) = 0.$$

Being that Γ_ϵ is a trajectory

$$\int_{\Gamma_\epsilon} (-y'\,\mathrm{d}x + x'\,\mathrm{d}y) = \int_{\Gamma_\epsilon} (-y'x' + x'y')\,\mathrm{d}t$$

so

$$\int_{\Gamma_\epsilon} (g_2(x,y)\,\mathrm{d}x - g_1(x,y)\,\mathrm{d}y) = 0.$$

We are operating under the assumption that Γ_ϵ is a perturbation of some solution Γ of an unperturbed equation; thus, the periodic orbit for the perturbed equation is close to the periodic orbit for the unperturbed equation Γ such that

$$\int_\Gamma (g_2(x,y)\,\mathrm{d}x - g_1(x,y)\,\mathrm{d}y) = 0.$$

Finally, we use Green's theorem for the closed solutions of the unperturbed equation and obtain

$$\iint_{int(\Gamma)} \left(\frac{\partial g_1}{\partial x} + \frac{\partial g_2}{\partial y} \right) \mathrm{d}x\,\mathrm{d}y = 0. \tag{3.7}$$

So we see that this integral must vanish if the perturbed trajectories are to be closed trajectories.

Now we will go through the procedure just outlined using the pendulum equation (3.2) as the unperturbed orbit and equation (2.1) as the perturbed orbit. We first recall our result from equation (3.3) that $H(x,y) = \frac{1}{2}y^2 - b\cos x$. Since H is constant on a given trajectory, (3.3) can be written without loss of generality as

$$A - b = \frac{1}{2}y^2 - b\cos x$$

where A is a constant. Solving for y yields

$$y = \pm\sqrt{2(A + b(\cos x - 1))}. \tag{3.8}$$

Now connecting back to our original equation we can identify g_1 and g_2 as outlined in equations (3.4) and (3.5) as 0 and $\cos x\, y$ respectively. Now to compute the integral from

(3.7), we need to find the limits of integration from the interior of the closed contour that (3.8) forms.

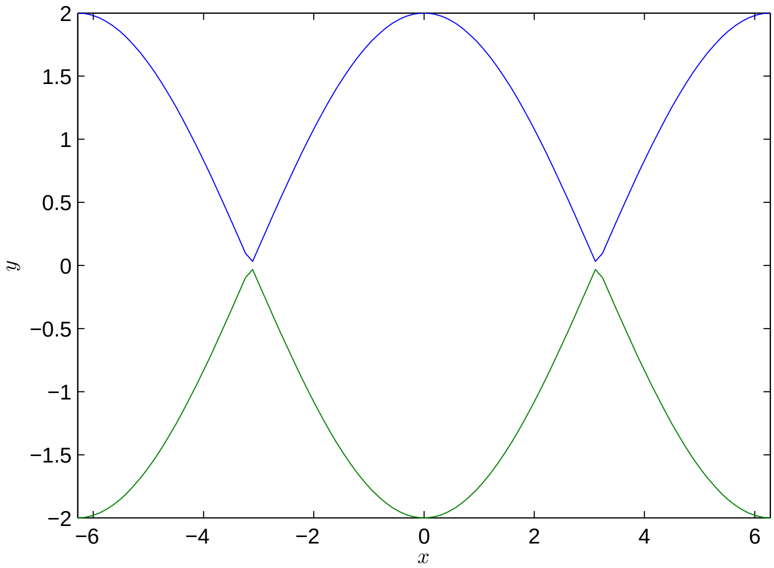

Figure 3.1: Plot of contour Γ from (3.8)

For illustration purposes we chose $A = 2$ and $b = 1$. From this numerical plot, the contour does not look closed, but it can be quickly verified that the contour is closed between -π and π. We can see that the upper and lower limits would be $\sqrt{2(A + b(\cos x - 1))}$ and $-\sqrt{2(A + b(\cos x - 1))}$ respectively, but we can make use of symmetry. To find the limits on x inside of the contour we let $y = 0$ and solve for x. After solving, we obtain $x = \pm \cos^{-1}\left(1 - \frac{A}{b}\right)$, but again we will use symmetry. Thus after differentiating, substituting, and inserting the limits of the double integral, equation (3.7) becomes

$$-4 \int_0^{\cos^{-1}\left(1-\frac{A}{b}\right)} \int_0^{\sqrt{2(A+b(\cos x-1))}} \cos x \, \mathrm{d}y \, \mathrm{d}x = 0.$$

Evaluating the first integral and dividing out unneeded constants gives

$$\int_0^{\cos^{-1}\left(1-\frac{A}{b}\right)} \cos x \sqrt{A + b(\cos x - 1)}\, \mathrm{d}x = 0. \tag{3.9}$$

The limits on this integral force the restriction $0 < A < 2b$ on A. A necessary and sufficient condition for periodic orbits is that we find a value of A that satisfies equation (3.9). With the parameter A appearing in both the integrand and the upper limit of the integral combined with an analytic nightmare as the integrand, the condition must be tested numerically.

We computed the integral in (3.9) in MATLAB using a function called AQGKIntegral which stands for Adaptive Quadrature Gauss-Kronrod Integration. The code for AQGK-Integral was obtained from L.F. Shampine, R.C. Allen, and S. Pruess' publication [11]. With AQGKIntegral we were able to, rather expensively, integrate numerically using A as a parameter. We rescaled the original differential equation so that $b = 1$ which made the computation simpler.

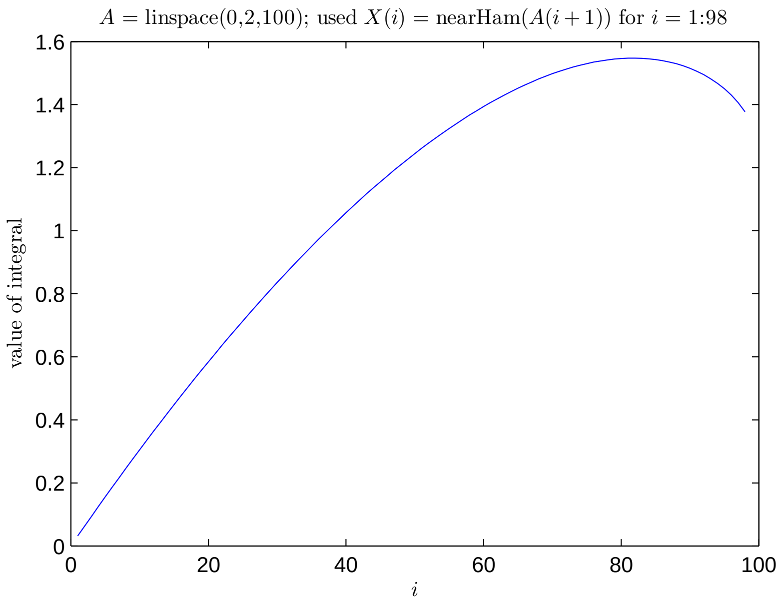

Figure 3.2: Integral from (3.9) evaluated for $0 < A < 2$

As was alluded to above, we required A to take on about one hundred values within the domain of A and used AQGKIntegral to evaluate (3.9) on each of those values, thus the horizontal axis refers not to the value of A, but the iteration of A on the interval $(0, 2)$. As Figure 3.2 indicates, the integral in equation (3.9) never takes on the value of zero for $0 < A < 2$. This leads us to conclude that although equation (2.1) bears a striking resemblance to other systems with periodic orbits it itself does not contain periodic orbits because it will not satisfy (3.6).

CHAPTER 4
PERTURBATION APPROXIMATIONS

4.1 Motivation

A.W. Bush [3] declares that "the governing equations of physical, biological and economic models often involve features which make it impossible to obtain their exact solutions"; this is true of the vortex motion equation that we have been analyzing throughout this paper. J.P. Keener [6] adds this statement, "At present one of the best hopes of solving (a problem that we do not know how to solve) occurs if it is "close" to another problem we already know how to solve. We study the solution of the simpler problem and then try to express the solution of the more difficult problem in terms of the simpler one modified by a small correction." In terms of the system expressed by equation (2.1), we wish to construct a system that preserves the properties discussed in the previous chapters, yet provide exact or approximate solutions, or at least yield to some attractive characteristics.

4.2 The van der Pol Equation

B.K Shivamoggi [12] proposed an approximation of equation (2.1) that would replace the trigonometric functions with polynomial functions. He did this by applying Taylor's Theorem to obtain the following.

$$\cos\theta \approx 1 - \frac{\theta^2}{2} \tag{4.1}$$

$$\sin\theta \approx \theta \tag{4.2}$$

Substituting (4.1) and (4.2) into equation (2.1) yields

$$\theta'' + a\left(1 - \frac{\theta^2}{2}\right)\theta' + b\theta = 0 \tag{4.3}$$

the van der Pol equation. The van der Pol equation certainly has some desirable properties and is easier to manipulate in many ways than the system that we began with.

We would like to find the equilibrium point(s), plot a phase plane, and discuss periodicity so that we can judge how good of an approximation equation (4.3) is to equation (2.1). We will make the same substitutions to find stability as we did in (2.2). After setting each first order equation equal to zero, we see that

$$\begin{aligned} 0 &= y \\ 0 &= a\left(1 - \tfrac{x^2}{2}\right)y - bx \end{aligned}.$$

Thus it is clear, since $b \neq 0$, that there is only one equilibrium solution $(0, 0)$. The Jacobian matrix for this system evaluated at the equilibrium point yields the zero matrix; hence, it is trivial to show that the nodes λ_k are both equal to zero. Figure 4.1 has been provided below to illustrate the phase plane of equation (4.3) when $a = 0.1$ and $b = 1$

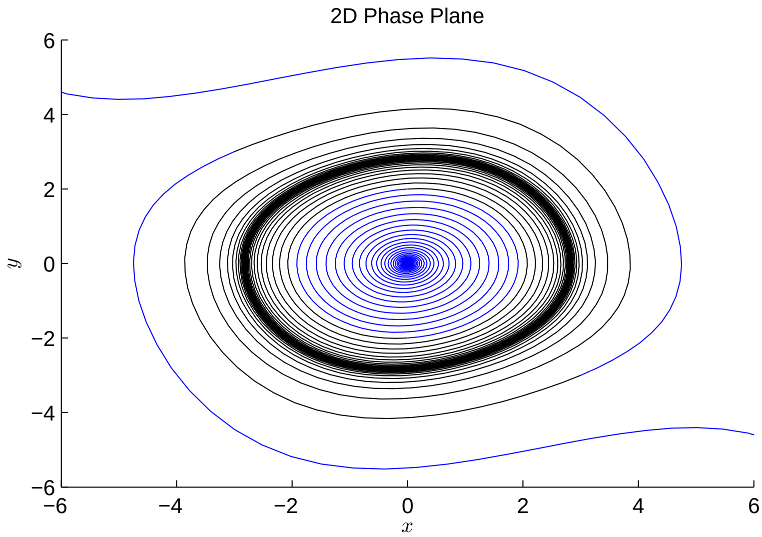

Figure 4.1: Phase plane of equation (4.3) van der Pol

In Simmons and Krantz [13] they conclude that since the van der Pol equation meets the conditions of Liénard's theorem, then equation (4.3) "has a unique closed path (periodic solution) that is approached spirally (asymptotically) by every other path (nontrivial solution)." We can see this in Figure 4.1. Thus, other than a critical point at the origin, the van der Pol equation does not seem to exhibit behavior or properties that would qualify it to be a good approximation of equation (2.1). Although equation (2.1) has only been a recent topic of interest, in the past (Shivamoggi, [12]) we have used the van der Pol equation for approximations; we now search for more accurate approximations.

4.3 Finding a Better Approximation

Between limit cycles, periodicity, critical points, and stability we concluded that the van der Pol equation should not be associated with equation (2.1) anymore; because of these unsatisfactory properties in the current approximation of equation (2.1), we began to search for a more suitable equation for approximation.

We observed in Section 4.2 that equation (4.3) was obtained by expanding the cosine and sine functions using Taylor polynomials. Note that (4.1) and (4.2) were only carried out to two terms and one term respectively. We could certainly take the polynomial representations of sine and cosine out to many more terms and obtain systems with incredible accuracy, but this would cost us the convenience of making an approximation in the first place. Instead let us try again only this time taking the sine term out to two terms rather than one. Thus we use

$$\sin\theta \approx \theta - \frac{\theta^3}{6}. \tag{4.4}$$

Hence, substituting (4.1) and (4.4) into equation (2.1)

$$\theta'' + a\left(1 - \frac{\theta^2}{2}\right)\theta' + b\left(\theta - \frac{\theta^3}{6}\right) = 0 \tag{4.5}$$

yields an equation that appears very similar to equation (4.3) which we have rejected as a good approximation. In fact, equation (4.5) is in some respect a combination of the Duffing equation and the van der Pol equation; it has the same damping term as the van der Pol equation while having the same oscillatory term as the Duffing equation.

As before, we find a system of first order differential equations and set each equation equal to zero

$$\begin{aligned} 0 &= y \\ 0 &= -a\left(1-\tfrac{x^2}{2}\right)y - b\left(x-\tfrac{x^3}{6}\right) \end{aligned}.$$

This time we reach more attractive results with respect to the original system; the equilibrium points are $(0,0)$ and $\left(\pm\sqrt{6},0\right)$. While the equilibrium points of equation (2.1) are $(n\pi,0)$, we can at least see similar behavior with this new approximation (4.5) for small values of x; whereas, the one critical point given from the van der Pol equation does not assist us in this manner.

4.3.1 Stability and Numeric Solutions

At the critical point $(0,0)$ we obtain the same results reached in Sections 2.1.1 and 2.1.2

$$\begin{aligned} 0 &= |J-\lambda I| \\ \lambda &= \frac{-a \pm \sqrt{a^2-4b}}{2}. \end{aligned}$$

Again, depending on the relationship between a and b and the positive or negative orientation of a, we will have two cases with two subcases; stable/unstable nodes and stable/unstable spirals. On the other hand, when we evaluate the Jacobian matrix

$$J = \begin{pmatrix} 0 & 1 \\ ayx - b + \frac{1}{2}bx^2 & -a + \frac{1}{2}ax^2 \end{pmatrix}$$

at the critical points $\left(\pm\sqrt{6}, 0\right)$ we obtain

$$J = \begin{pmatrix} 0 & 1 \\ 2b & 2a \end{pmatrix}. \tag{4.6}$$

As we find the eigenvalues associated with (4.6)

$$\begin{aligned} 0 &= |J - \lambda I| \\ \lambda &= a \pm \sqrt{a^2 + 2b} \end{aligned}$$

we see that, much like the results in Section 2.1.3, saddle points will form at these critical points. Let us illustrate the results just found via phase plane portraits of equation (4.5) for both positive and negative values of a.

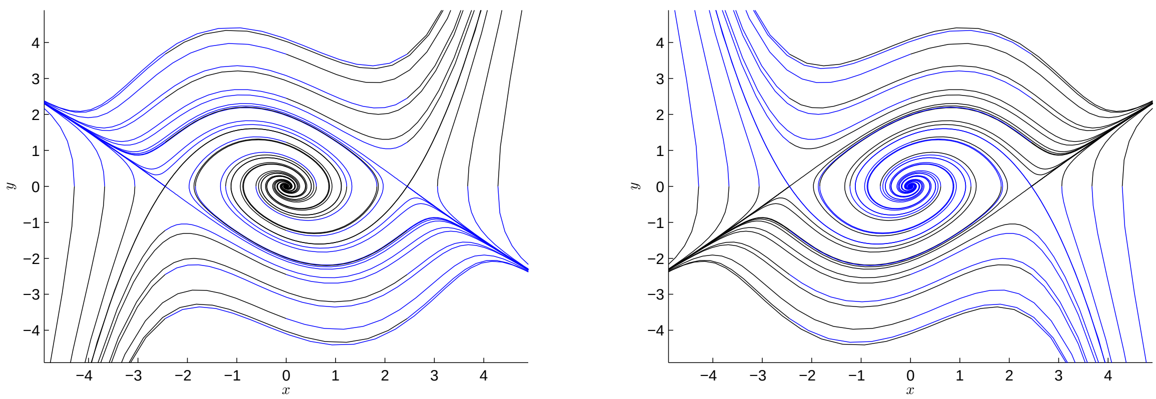

(a) $a > 0$ (b) $a < 0$

Figure 4.2: Phase plane of equation (4.5) where $a = \pm\frac{1}{2}$, $b = 1$; $4b > a^2$

While equation (4.5) only has three critical points, each of them exhibits the same type of behavior as the corresponding critical points of equation (2.1), $(0, 0)$ and $(\pm\pi, 0)$. From

Figure 4.2 we do see that as we move out to larger values of x, the approximation is no longer helpful; this is to be expected from approximations obtained from Taylor expansions. Because of this we will want to restrict such approximations to small values of x.

4.3.2 Analytic Solutions

While the numerical results found in Section 4.3.1 are helpful in determining the relationship between equations (2.1) and (4.5), in Section 4.1 we noted that our interest in approximations stemmed from a curiosity of the analytic solutions of the original system. We will begin by considering the following initial valued perturbation approximation of equation (2.1)

$$\begin{cases} \frac{\mathrm{d}^2\theta}{\mathrm{d}s^2} + \epsilon a\left(1 - \frac{\theta^2}{2}\right)\frac{\mathrm{d}\theta}{\mathrm{d}s} + b\left(\theta - \frac{\theta^3}{6}\right) = 0, \quad a \neq 0, b > 0 \\ \theta(0) = \epsilon \qquad \theta'(0) = 0 \end{cases} . \tag{4.7}$$

Initially we tried substituting the standard expansion

$$\theta = \theta_0 + \epsilon\theta_1 + \epsilon^2\theta_2 + O\left(\epsilon^3\right),$$

but that led to contribution of the nonlinear term $-\frac{b}{6}\theta^3$. Instead we chose θ_0 to be zero so that the lowest order equation would be linear

$$\theta = \epsilon\theta_1 + \epsilon^2\theta_2 + O\left(\epsilon^3\right); \tag{4.8}$$

however, the straightforward two-term expansion

$$\theta = \epsilon\cos\left(\sqrt{b}s\right) + \frac{\epsilon^2 a}{2}\left[\frac{1}{\sqrt{b}}\sin\left(\sqrt{b}s\right) - s\cos\left(\sqrt{b}s\right)\right] \tag{4.9}$$

yielded nonuniformities because of the secular term $s\cos\left(\sqrt{b}s\right)$ that was introduced. In order to eliminate such nonuniformities we introduce the method of multiple scales; we will use two space scales

$$S_0 = s \text{ and } S_1 = \epsilon s. \tag{4.10}$$

We must first change the derivatives from equation (4.8) to time derivatives

$$\begin{array}{r}\frac{\mathrm{d}}{\mathrm{d}s} = \frac{\partial}{\partial S_0} + \epsilon\frac{\partial}{\partial S_1} \\ \frac{\mathrm{d}^2}{\mathrm{d}s^2} = \frac{\partial^2}{\partial S_0^2} + 2\epsilon\frac{\partial^2}{\partial S_0 \partial S_1} + \epsilon^2\frac{\partial^2}{\partial S_1^2}\end{array}. \tag{4.11}$$

Now substituting (4.11) into (4.7) we have

$$\frac{\partial^2\theta}{\partial S_0^2} + 2\epsilon\frac{\partial^2\theta}{\partial S_0\partial S_1} + \epsilon^2\frac{\partial^2\theta}{\partial S_1^2} + \epsilon a\left(1-\frac{\theta^2}{2}\right)\left(\frac{\partial\theta}{\partial S_0} + \epsilon\frac{\partial\theta}{\partial S_1}\right) + b\left(\theta - \frac{\theta^3}{6}\right) = 0 \tag{4.12}$$

Now we will use the substitution from (4.8) to obtain the following set of equations

$$O(\epsilon): \quad \frac{\partial^2\theta_1}{\partial S_0^2} + b\theta_1 = 0 \tag{4.13}$$

$$O\left(\epsilon^2\right): \quad \frac{\partial^2\theta_2}{\partial S_0^2} + b\theta_2 = -2\frac{\partial^2\theta_1}{\partial S_0\partial S_1} - a\frac{\partial\theta_1}{\partial S_0} \tag{4.14}$$

$$O\left(\epsilon^3\right): \quad \frac{\partial^2\theta_3}{\partial S_0^2} + b\theta_3 = -2\frac{\partial^2\theta_2}{\partial S_0\partial S_1} - a\frac{\partial\theta_2}{\partial S_0} - \frac{\partial^2\theta_1}{\partial S_1^2} - a\frac{\partial\theta_1}{\partial S_1} \tag{4.15}$$

The solution of the homogenous partial differential equation (4.13) is

$$\theta_1 = A(S_1)\cos\left(\sqrt{b}S_0\right) + B(S_1)\sin\left(\sqrt{b}S_0\right). \tag{4.16}$$

Substituting (4.16) into equation (4.14) gives

$$\frac{\partial^2\theta_2}{\partial S_0^2} + b\theta_2 = 2\sqrt{b}\left[\frac{\mathrm{d}A}{\mathrm{d}S_1}\sin\left(\sqrt{b}S_0\right) - \frac{\mathrm{d}B}{\mathrm{d}S_1}\cos\left(\sqrt{b}S_0\right)\right] + a\sqrt{b}\left[A\sin\left(\sqrt{b}S_0\right) - B\cos\left(\sqrt{b}S_0\right)\right]$$

$$\frac{\partial^2\theta_2}{\partial S_0^2} + b\theta_2 = \sqrt{b}\left[\left(2\frac{\mathrm{d}A}{\mathrm{d}S_1} + aA\right)\sin\left(\sqrt{b}S_0\right) - \left(2\frac{\mathrm{d}B}{\mathrm{d}S_1} + aB\right)\cos\left(\sqrt{b}S_0\right)\right] \tag{4.17}$$

At this point we realize that should we solve this equation as it stands, then we would introduce secular terms of the form $s\sin\left(\sqrt{b}S_0\right)$ or $s\cos\left(\sqrt{b}S_0\right)$. The following requirements will ensure that our expansion remains uniformly valid

$$2\frac{\mathrm{d}A}{\mathrm{d}S_1} + aA = 0 \quad \text{and} \quad 2\frac{\mathrm{d}B}{\mathrm{d}S_1} + aB = 0$$

Solving these linear differential equations yields

$$\begin{aligned} A(S_1) &= c_1 e^{-\frac{1}{2}aS_1} \\ B(S_1) &= c_2 e^{-\frac{1}{2}aS_1} \end{aligned}.$$

After applying the initial conditions $A(0) = 1$ and $B(0) = 0$ we determine that $c_1 = 1$ and $c_2 = 0$. This condenses equation (4.17) to a homogenous equation with the following solution

$$\theta_2 = C(S_1)\cos\left(\sqrt{b}S_0\right) + D(S_1)\sin\left(\sqrt{b}S_0\right).$$

Thus we can be sure that the solution

$$\theta = \epsilon e^{-\frac{1}{2}aS_1}\cos\left(\sqrt{b}S_0\right) + O\left(\epsilon^2\right)$$

is uniformly valid for $s = O(1/\epsilon)$. At this stage we may back substitute from (4.10) to obtain

$$\theta = \epsilon e^{-\frac{1}{2}a\epsilon s}\cos\left(\sqrt{b}s\right) + O\left(\epsilon^2\right). \tag{4.18}$$

Such a solution makes sense in terms of our original system (2.1) because we see the unstable growth for $a < 0$ as well as the stable decay when $a > 0$.

4.4 Other Approximations

Equation (4.7) is certainly a system that better exemplifies the characteristics of equation (2.1) than the current approximation in the van der Pol equation, but it is not the only approximation worthy of mention. Consider making the substitution $u = \sin\theta$ in equation (2.1). After applying the chain rule in order to make the change of variable we obtain

$$\frac{\mathrm{d}\theta}{\mathrm{d}s} = \frac{1}{\sqrt{1-u^2}}\frac{\mathrm{d}u}{\mathrm{d}s} \tag{4.19}$$

and

$$\frac{\mathrm{d}^2\theta}{\mathrm{d}s^2} = \frac{1}{\sqrt{1-u^2}}\frac{\mathrm{d}^2u}{\mathrm{d}s^2} + \frac{u}{\sqrt{(1-u^2)^3}}\left(\frac{\mathrm{d}u}{\mathrm{d}s}\right)^2. \tag{4.20}$$

Now substituting u as well as equations (4.19) and (4.20) into equation (2.1) we obtain

$$\left(1-u^2\right)^{-1/2}u'' + u\left(1-u^2\right)^{-3/2}u'^2 + au' + bu = 0 \tag{4.21}$$

where prime denotes differentiation with respect to s. We can rewrite (4.21) as

$$u'' + u\left(1-u^2\right)^{-1}u'^2 + a\left(1-u^2\right)^{1/2}u' + bu\left(1-u^2\right)^{1/2} = 0. \tag{4.22}$$

Recalling from the Binomial Theorem that $(a+b)^r \approx a^r + ra^{r-1}b$, we express (4.22) as

$$u'' + uu'^2 + a\left(1-\frac{1}{2}u^2\right)u' + bu\left(1-\frac{1}{2}u^2\right) + O(u^3) = 0. \tag{4.23}$$

Following the processes outlined several times in this paper we observe the following results about equation (4.23): the critical points are $(0,0)$ and $(\pm\sqrt{2},0)$, the eigenvalues associated with $(0,0)$ are the same as that of (2.9), and the eigenvalues associated with

$(\pm\sqrt{2}, 0)$ are $\lambda_1 = -\sqrt{2b}$ and $\lambda_2 = \sqrt{2b}$. Each critical point and eigenvalue leads to the same properties as equation (2.1) in terms of types and form of stability.

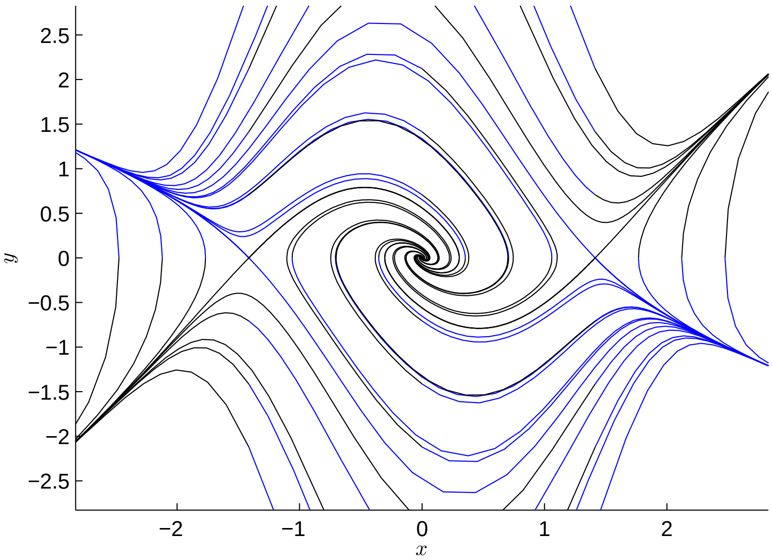

Figure 4.3: Phase plane of equation (4.23) where $a = 1$, $b = 1$; $\quad 4b > a^2$

Figure 4.3 exhibits behavior qualitatively similar to the original system for small values of x. It seems that equation (4.5) is a better approximation quantitatively than equation (4.23) because the critical points of (4.5) are closer to the original's points. Finally taking a to be small and imposing initial conditions we can rewrite equation (4.23) as

$$\begin{cases} \frac{\mathrm{d}^2 u}{\mathrm{d}s^2} + u\left(\frac{\mathrm{d}u}{\mathrm{d}s}\right)^2 + \epsilon a\left(1 - \frac{1}{2}u^2\right)\left(\frac{\mathrm{d}u}{\mathrm{d}s}\right) + bu\left(1 - \frac{1}{2}u^2\right) = 0, \quad a \neq 0, b > 0 \\ u(0) = \epsilon \qquad u'(0) = 0 \end{cases} .$$

Following the method of multiple scales previously demonstrated, we obtain this solution

$$u = \epsilon e^{-\frac{1}{2}a\epsilon s} \cos\left(\sqrt{b}s\right) + O\left(\epsilon^2\right)$$

which is uniformly valid for $s = O(1/\epsilon)$. After back substitution we obtain

$$\theta = \arcsin\left[\epsilon e^{-\frac{1}{2}a\epsilon s}\cos\left(\sqrt{b}s\right)\right] + O\left(\epsilon^2\right). \tag{4.24}$$

CHAPTER 5
CONCLUDING REMARKS

In this paper we have thoroughly researched the mathematical properties of the topic of rotating vortex filament in superfluid ^{4}He. We now know what to expect in terms of stability for different values of θ, the angle between the tangent to the vortex filament and the x-axis. We can also note that when the damping coefficient α is not equal to zero, and if the normal fluid velocity is in the same direction as vorticity in the undisturbed vortex $\alpha U_1 > 0$, then there is growth of the vortex line length. In contrast, when the normal velocity is in the opposite direction $\alpha U_1 < 0$, then there is decay of the vortex line length.

We have also shown that the system of interest does not have periodic solutions unless the damping coefficient α or the normal fluid velocity U_1 is equal to zero; in such a case periodic vortex shape is possible. This knowledge aided us in determining that the van der Pol equation is not a sufficient approximation for our system.

Potentially most importantly we found two systems, equations (4.5) and (4.23), that preserve the qualities of the original system in a satisfactory way. In connection with these perturbation approximations we found analytic solutions which may serve to be of use in future research regarding this system.

On the note of approximations and future research, one may consider several options. The initial values that we chose while preforming perturbation expansions led to fitting results while others did not; it is possible that there are other initial values that will also produce analytic solutions. In research we used two space scales in solving our perturbed systems as well as three space scales. The latter did not seem to lend to any particularly interesting results, but it did introduce nonlinear terms in the $O\left(\epsilon^3\right)$ equations. We have verified that these nonlinear terms do not introduce any nonuniformities, but we have not investigated in detail its effects on the analytic solutions. Also one may try using a different substitution or attempt expanding the trigonometric functions beyond the first two terms from their respective Taylor series representations in order to find new approximations.

Beyond a search for better approximations, one may explore the physical implications of the approximations already discussed as well as the associated analytic solutions which we obtained. We have explored, in a rudimentary sense, the effects of positive and negative friction coefficients and normal fluid velocity in our analytic solutions and verified that they produce the desired results, but further interpretation may very well be helpful in future physical research.

LIST OF REFERENCES

[1] L.C. Andrews and R.L. Phillips, *Mathematical Techniques for Engineers and Scientists*, SPIE PRESS, Bellingham, Washington, 2003.

[2] B. Bunch and A. Hellemans, *The History of Science and Technology: A Browser's Guide to the Great Discoveries, Inventions, and the People Who Made Them from the Dawn of Time to Today*, Houghton Mifflin Company, New York, New York, 2004.

[3] A.W. Bush, *Perturbation Methods for Engineers and Scientists*, CRC Press, Inc., Boca Raton, Florida, 1992.

[4] P. Glendinning, *Stability, Instability and Chaos: An Introduction to the Theory of Nonlinear Differential Equations*, Cambridge University Press, Cambridge, United Kingdom, 1994.

[5] R. Grimshaw, *Nonlinear Ordinary Differential Equations*, CRC Press LLC, Boca Raton, Florida, 1993.

[6] J.P. Keener, *Principles of Applied Mathematics: Transformations and Approximation*, Westview Press, Cambridge, Massachusetts, 2000.

[7] I. Kroo, *Applied Aerodynamics: A Digital Textbook*, Desktop Aeronautics, Inc., Stanford, California, 2007.

[8] H. Lamb, *Hydrodynamics*, Cambridge University Press, London, England, 1895.

[9] R. Larson, R.P. Hostetler, and B.H. Edwards, *Calculus with Analytic Geometry*, Houghton Mifflin Company, Boston, Massachusetts, 2002.

[10] A. Leitner, *Liquid Helium II the Superfluid*, [Video], Michigan State University, 1963.

[11] L.F. Shampine, R.C. Allen, and S. Pruess, *Fundamentals of Numerical Computing*, John Wiley & Sons, Inc., Hoboken, New Jersey, 1997.

[12] B.K. Shivamoggi, *Effects of Friction Force on the Vortex Motion in Superfluid* ^4He, ArXiv e-prints **0909.3799** (2009), 1–11.

[13] G.F. Simmons and S.G. Krantz, *Differential Equations: Theory, Technique, and Practice*, The McGraw-Hill Companies, Inc., New York, New York, 2007.

[14] D.S. Viswanath, T.K. Ghosh, D.H.L. Prasad, N.V.K. Dutt, and K.Y. Rani, *Viscosity of Liquids: Theory, Estimation, Experiment, and Data*, Springer, Dordrecht, The Netherlands, 2007.

[15] G.E. Volovik, *Exotic Properties of Superfluid* ^3He, World Scientific Publishing Co. Pte. Ltd., River Edge, New Jersey, 1992.